

SLAST Shower Initiated Light Attenuated to the Space Telescope

Dmitry V. Naumov

*LAPP**

(Dated: April 16, 2003)

This document is a short description of both physics and user event simulation of fluorescent and cherenkov light signals produced by a high energy shower initiated by cosmic rays. Also this note describes some results of the simulation made using SLAST.

PACS numbers:

Contents

I. Introduction	1
II. Physics ingredients	1
A. Atmosphere profiles	2
B. First Interaction	2
1. Nuclei	2
2. (Anti) Neutrinos	3
C. Shower development	3
1. Number of electrons	3
2. Energy distribution of electrons in shower	3
D. Fluorescent light	4
E. Cherenkov light	4
F. Atmosphere attenuation	5
III. Analysis	6
A. Detection Efficiencies	6
B. Photons Arrived to EUSO	7
C. Proton/Neutrino discrimination	8
D. Expected Statistics	8
IV. Steering the simulations	9
A. Code maintenance and general agreements	10
B. Compilation	10
C. Running	11
D. SLAST output	11
Acknowledgments	11
A. Column Wise Ntuple Structure	12
References	12

I. INTRODUCTION

Recent years are marked by an increasing interest to Ultra High Energy Cosmics Rays (UHECR) Physics and various UHECR detection techniques are proposed both from the ground like Auger [1] and from the Space like

EUSO [2] or KLYPVE/TUS [3] projects. Space Based Missions are in R&D stage now which means a study of the detector performance and its optimization. Such studies need a fast generator of showers. SLAST is being developed just for this purpose. This is a fast shower generator which uses parametrization of the data and/or extensive shower generators thus loosing some details while keeping all important effects. SLAST is able to generate showers initiated by various nuclei or (anti) neutrino. The initial interaction point of nuclei is taken according to nuclei-Air cross section parametrization and extrapolation of existing data. Θ and ϕ are taken randomly according to uniform distribution (later in the analysis stage one can easily put the appropriate weight), energy of the initial particle is also taken randomly. User can always define an interval of variation of these parameters. Electrons and positrons of the shower produce both fluorescent and the cherenkov light which could arrive to the Space Telescope.

The software is organized in such a way that one can test various models of the atmosphere profile, shower parametrization, fluorescent yield parametrization, space telescope key parameters, etc without recompilation.

This note is organized as follows. Sec. II summarizes physical ingredients adopted within SLAST. Some results of the simulation one can find in Sec. III. In Sec. IV I explain all details of the software maintenance, its installation and use.

II. PHYSICS INGREDIENTS

This section summarizes all the physics ingredients used to cook SLAST:

- A Atmosphere profile
- B First interaction
- C Shower development
- D Fluorescence yield
- E Cherenkov photons
- F Attenuation

*Joint Institute for Nuclear Research, Dubna, 141980, Russia; Electronic address: naumov@lapp.in2p3.fr

A. Atmosphere profiles

The atmosphere and the Earth are both spherical in the SLAST framework. The following density profiles are tabulated inside SLAST:

- Isothermic atmosphere (user has a possibility to set its temperature via global.datacard, see Sec. IV).
- US 1976 Standard atmosphere

It is easy and straightforward to add any other atmosphere profile in case of need. The atmosphere density profiles are compared to each other in Fig. 1. This comparison implies that the adopted atmosphere profiles are very well consistent with each other.

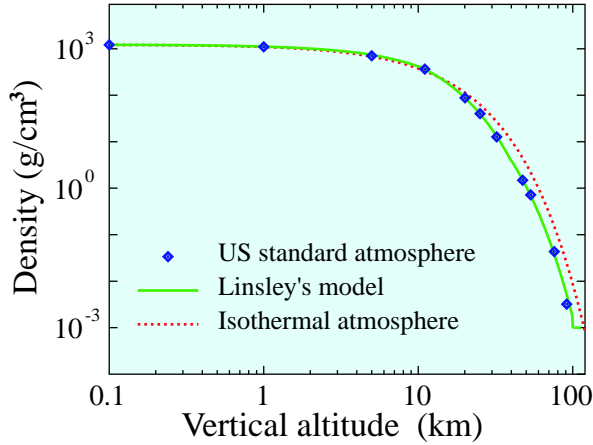


FIG. 1: Density profile for Isothermic atmosphere, US 1976 Standard atmosphere and Linsley model.

Let us introduce a variable x called depth. The depth definition is the mass of the material within a volume of 1cm^2 cross-section and length dl :

$$dx = \rho dl.$$

Let us $x(h, \Theta)$ be the atmosphere depth from a point with altitude h along Θ direction up to ∞ [4]:

$$x(h, \Theta) = \int_h^\infty dh' \rho(h') \left(1 - \sin^2 \Theta \left(\frac{R_\oplus + h}{R_\oplus + h'} \right)^2 \right)^{-1/2}.$$

Thus the atmosphere depth between two points with altitudes h_1, h_2 and two zenith angles Θ_1, Θ_2 (which are slightly different from the incident zenith angle Θ due to the atmosphere sphericity) is:

$$x(h_1, \Theta_1; h_2, \Theta_2) = |x(h_1, \Theta_1) - x(h_2, \Theta_2)|.$$

To speed up the event generation SLAST precomputes depth integrals for adopted atmosphere profiles and later uses precomputed tables.

Fig. 2 could help to understand the above definitions and the equations. Both Fig. 1, 2 are courtesy of V.A.Naumov.

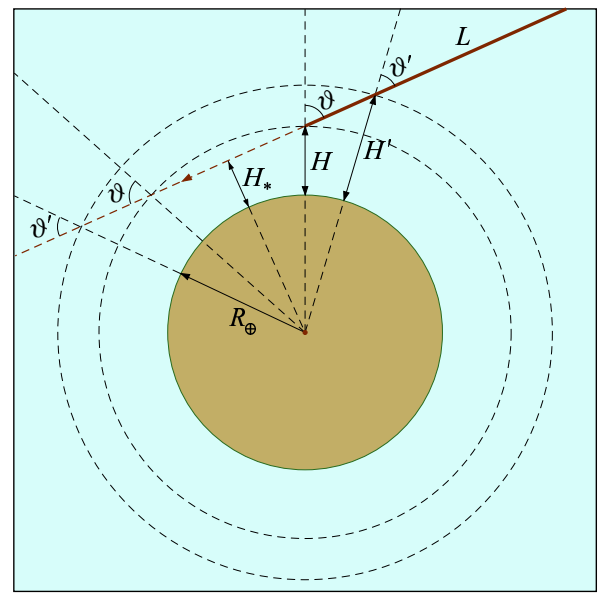


FIG. 2: Spherical Earth and the Atmosphere

B. First Interaction

Arrival direction is simulated isotropical. In the analysis stage one should use an appropriate weight ($\sim \sin \Theta$). The first depth simulation is quite different for nuclei and neutrinos:

- mean value of the atmospheric depth for protons with $E = 10^{20}$ eV is about $35\text{-}40 \text{ g/cm}^2$. This makes possible a direct simulation of the first interaction depth thus directly giving (with Θ and ϕ simulated) the first interaction point.
- However for neutrinos the Standard Model extrapolation predicts $\sigma \approx 10^{-31} \text{ cm}^2$ thus giving the mean value of the atmospheric depth to be about 10^7 g/cm^2 which is significantly larger than the horizontal atmospheric depth ($\approx 35000 \text{ g/cm}^2$) [15].

1. Nuclei

The first interaction depth (x_1) is taken randomly according to

$$e^{-x_1/x_0} \text{ distribution,}$$

where $x_0 = \langle A_{air} \rangle / (\sigma N_A)$. Here $\langle A_{air} \rangle$ is the mean atomic mass value (for air $\langle A_{air} \rangle = 14.483$), σ is the nucleus-air cross section, and N_A is the Avogadro number.

The proton-air cross section is given by [5]:

$$\sigma_{pAir}(E) = \sigma_0 - \Theta(E - E_*) (\sigma_1 \ln(E/E_1) - \sigma_2 \ln^2(E/E_1)), \quad (1)$$

where $\sigma_0 = 290 \pm 5 \text{ mbarn}$, $\sigma_1 = 8.7 \pm 0.5 \text{ mbarn}$, $\sigma_2 = 1.14 \pm 0.05 \text{ mbarn}$, $E_* = 45.4 \text{ GeV}$, $E_1 = 1 \text{ GeV}$.

To calculate nucleus air cross section at least two effects should be taken into account: energy carried by nucleons is reduced $E \rightarrow E/A$ and the effective cross sec-

tion is increased in respect to proton-air interaction. We adopted the following parametrization [5]:

$$\sigma_{AAir} = \pi R_0^2 \sum_{i=N_2, O_2, Ar, CO_2} C_i \left(m_i^{1/3} + A^{1/3} - 0.93 \left(m_i^{-1/3} + A^{-1/3} \right)^2 \right) \frac{\sigma_{pAir}(E/A)}{\sigma_{pAir}(10^{11} \text{ eV}/A)}, \quad (2)$$

where $R_0 = 1.28710^{-13}$ cm, C_i is the relative concentration of N_2, O_2, Ar, CO_2 in air, m_i is atomic mass of these species. The fraction $\sigma_{pAir}(E/A)/\sigma_{pAir}(10^{11} \text{ eV}/A)$ is used to have a proper energy dependence for σ_{AAir} [4].

2. (Anti) Neutrinos

The (anti) neutrino cross sections are parametrized according to [6]. We simulate (anti) neutrino first interaction point directly with its altitude proportional to the air density[7].

C. Shower development

1. Number of electrons

An analytical formula generalizing Rossi and Greisen [10] parametrization of photon induced showers and Ilina, Kalmykov and Prosin parametrization of nucleus initiated showers [11] was proposed by Linsley in 2001. This formula being basically an analytical approximation of the longitudinal shower development of QGSJET model by Kalmykov and Ostapchenko [12] is known however as GIL parametrization. We will keep using this name as well however giving credits to its real authors. According to GIL formula the number of electrons and positrons in EAS is given by:

$$N_e = \frac{E}{E_1} e^{f(t)}, \quad (3)$$

where E is the energy of the incident particle, $E_1 = 1.45 \text{ GeV}$, and $f(t) = t - t_{max} - 2t \ln s$. $t = \frac{x}{x_0}$ (x is the atmosphere depth at the given point of the shower development, $x_0 = 37.15 \text{ g/cm}^2$ is the air radiation length), $t_{max} = a + b(\ln(\frac{E}{E_0}) - \ln A)$ (with $E_0 = 81 \text{ MeV}$, and A being the atomic number of an incident nuclei) and $s = \frac{2}{1 + t_{max}}$ (the shower age). Fig. 3 displays the number of electrons as a function of depth for proton and iron initiated showers in GIL parametrization at $E = 10^{20} \text{ eV}$.

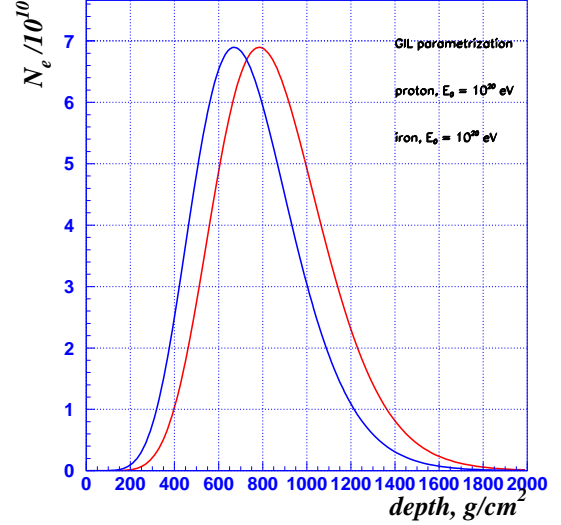


FIG. 3: Number of electrons as a function of depth for proton and iron initiated showers in GIL parametrization at $E = 10^{20} \text{ eV}$

2. Energy distribution of electrons in shower

The energy distribution of electrons in shower is important for both the fluorescence and the cherenkov light production. We adopted the Hillas parametrization of his MC simulation for the fraction of charged particles with energy above e [13]:

$$T(e) = \left(\frac{0.89e_0 - 1.2}{e_0 + e} \right)^s (1 + 10^{-4}se)^{-2}, \quad (4)$$

where

$$e_0 = \begin{cases} 44 - 17(s - 1.46)^2 & \text{for } s \geq 0.4 \\ 26 & \text{for } s < 0.4 \end{cases}$$

Energy unit here is MeV. From (4) I derived the energy distribution of electrons in shower:

$$f(e, s) = -\frac{dT(e)}{de} = \frac{10^8 \left(\frac{0.89e_0 - 1.2}{e_0 + e} \right)^8 \cdot s \cdot (10^4 + 2e_0 + e(2 + s))}{(e + e_0)(10^4 + es)^3} \quad (5)$$

D. Fluorescent light

The fluorescent light can be produced by charged particles passing in air and exciting N_2 molecules (2P band) and N_2^- ions (1N band). This light is emitted isotropically. The fluorescent yield (Y) in (300,400) nm band is approximately 4-5 photons per electron per meter. However Y is a rather complex function which depends on air density, temperature and composition.

SLAST adopts the following parametrization for the integral yield of fluorescent photons [8]:

$$Y(h) = \frac{dE/dx}{(dE/dx)_{1.4 \text{ MeV}}} \rho \left[\frac{A_1}{1 + \rho B_1 \sqrt{T}} + \frac{A_2}{1 + \rho B_2 \sqrt{T}} \right], \quad (6)$$

where dE/dx is the ionization energy loss of electrons

in air[16], ρ - air density in kg/m^3 , T - temperature in K. The parameters values are: $A_1 = 89.0 \pm 1.7 \text{ m}^2\text{kg}^{-1}$, $B_1 = 1.85 \pm 0.04 \text{ m}^3\text{kg}^{-1}\text{K}^{-1/2}$, $A_2 = 55.0 \pm 2.2 \text{ m}^2\text{kg}^{-1}$, $B_2 = 6.50 \pm 0.33 \text{ m}^3\text{kg}^{-1}\text{K}^{-1/2}$.

The relative intensities of lines are taken from [9] and are displayed in Fig. 4. Since the fluorescence yield depends on the particle energy this results in its dependence on the shower age. Eqs. (7) shows the adopted parametrization. Efficiencies are taken from [9] for ϵ^{DON} and from [8] for ϵ^K . I do not use [8] parametrization below 1.4 MeV since there is no measurement there. Instead I use [9] renormalized yield. Hopefully it does not change too much the fluorescent yield due to a small contribution of (0,1.4) MeV region in the shower energy distribution.

$$Yield(s, h) = w(s) \cdot Y(h),$$

$$w(s) = \frac{1}{Norm(s)} \int_{1.4 \text{ MeV}}^{\infty} f(e, s) \frac{dE/dx}{(dE/dx)_{1.4 \text{ MeV}}} de + \frac{\sum_i \epsilon^{DON}(\lambda_i)}{\sum_i \epsilon^K(\lambda_i)} \int_0^{1.4 \text{ MeV}} f(e, s) de \quad (7)$$

$$Norm(s) = \int_0^{\infty} f(e, s) de$$

The fluorescence yield as a function of the altitude in the atmosphere and the shower age is shown in Fig. 4. There is an evident decrease of the fluorescence yield within the shower age due to decrease of the mean energy of electrons for “old” shower.

The number of fluorescent photons produced by the shower and arrived to EUSO entrance pupil during one GTU (Gait Time Unit) is given by:

$$N_{fl} = \Delta\Omega Yield(s, h) \eta(\mathbf{R}, \mathbf{ISS}) N_e(x) \Delta L, \quad (8)$$

where $\Delta\Omega$ is the EUSO solid angle from the emission point, $Yield(s, h)$ is the fluorescence yield as a function of the shower age (s) and the altitude in the atmosphere (h), $\eta(\mathbf{R}, \mathbf{ISS})$ is the atmosphere attenuation between \mathbf{R} and \mathbf{ISS} (\mathbf{ISS}), $N_e(x)$ is the number of electrons in the shower, and ΔL is the track length corresponding to one GTU. Note, that ΔL is not just a number rather this is a function of the UHECR arrival direction and the photon emission point:

$$\Delta L = \frac{c \cdot GTU}{1 + \mathbf{n} \cdot \mathbf{\Omega}}, \quad (9)$$

where \mathbf{n} is the unit vector pointing to EUSO from the shower maximum, and $\mathbf{\Omega} = (\sin \Theta \cos \phi, \sin \Theta \sin \phi, \cos \Theta)$ is the arrival direction of the shower.

E. Cherenkov light

The cherenkov photons are produced by charged particles due to $n \neq 1$ in air. A classical theory gives the number of cherenkov photons produced by N_e electrons on dl path to be:

$$\frac{dN_{ch}}{dl} = 4\pi\alpha\delta N_e \int_{\lambda_{min}}^{\lambda_{max}} d\frac{1}{\lambda} \int_{E_{th}}^{\infty} f(E) \left(1 - \left(\frac{E_{th}}{E} \right)^2 \right) dE, \quad (10)$$

where $\delta = n - 1$, $E_{th} = mc^2/\sqrt{2\delta}$ is the energy threshold for electrons for the cherenkov light production. Qualitatively within isothermic model each electron with energy above the threshold produces about:

$$18 e^{-h/H_0} \text{ photons per meter,}$$

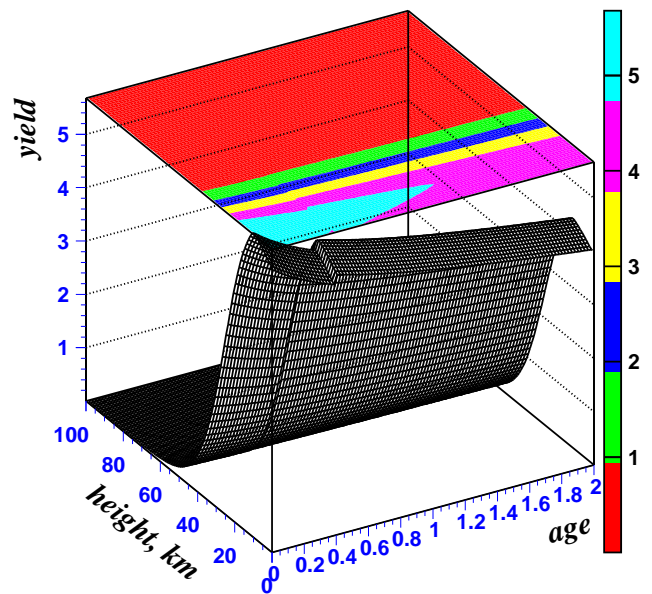
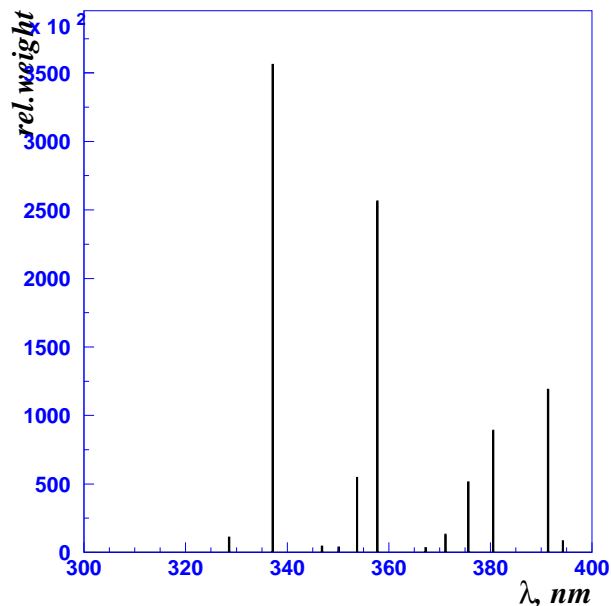


FIG. 4: Relative intensities of fluorescent lines from [9] (left). The fluorescence yield as a function of the altitude in the atmosphere and the shower age (right).

while the energy threshold grows with altitude exponentially:

$$E_{th} = 23 e^{h/2H_0} \text{ MeV}.$$

The exponential grow of the energy threshold for the cherenkov light production drastically suppresses a number of produced cherenkov photons at large Θ for proton

initiated showers. Say, at $\Theta = 50^\circ$ altitude of the shower maximum is about 4 kms, which gives $E_{th} = 42$ MeV, and at $\Theta = 80^\circ$ $E_{th} = 157$ MeV is above the mean energy of the electrons in shower.

To compute the number of cherenkov photons arrived to EUSO SLAST finds $\int dN_{ch}(\mathbf{R}) \eta(\mathbf{R}, \mathbf{Ground})$ over all path which is multiplied by:

$$N_{ch} = \int dN_{ch}(\mathbf{R}) \eta(\mathbf{R}, \mathbf{Ground}) \times \Delta\Omega \times \eta(\mathbf{Ground}, \mathbf{ISS}) \times Albedo,$$

where $\Delta\Omega$ is the EUSO solid angle from the hitted point at the ground (\mathbf{Ground}), $\eta(\mathbf{R}, \mathbf{Ground})$ is the attenuation function from the ground point to EUSO, $Albedo$ is the Earth Albedo. The surface is assumed to be Lambertian, which means a not uniform distribution of reflected light, rather it has the following form:

$$Albedo = Albedo_0 \cos(\Theta),$$

with $Albedo_0 = 0.05$ and Θ is the angle between the normal to the surface and the cherenkov light.

Please, note that currently SLAST does not take into account the time dispersion of the cherenkov light due to a non-zero emission angle of the cherenkov light. However in the analysis section (see Sec. III) we take this into account computing a “spread function”. Fig. 5 can

give you an idea of importance of this effect for inclined showers.

F. Atmosphere attenuation

The atmosphere plays the dramatical role in the light absorption and its deflection. These effects (together with clouds and other “imperfections” of the atmosphere) should be taken into account simulating and analysing data. For the control and cross-checks SLAST follows two ways to account for the atmosphere effects:

1. Analytic description of Rayleigh and Mie scattering
2. LOWTRAN7.1 more sophisticated algorithm.

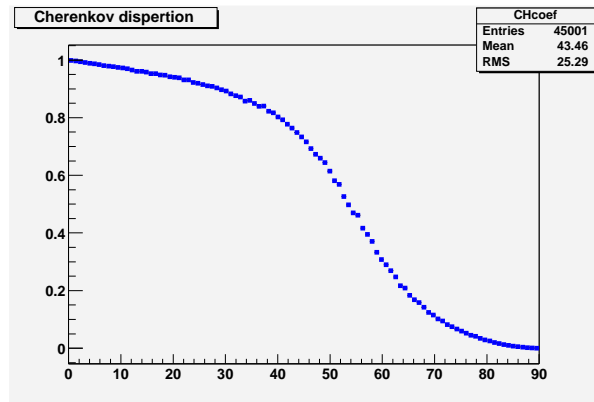


FIG. 5: Spread function for the cherenkov light due non zero emission angle of the cherenkov light. The x-axis is the UHECR zenith angle in degrees.

Rayleigh scattering

The transition coefficient between two points in the atmosphere \mathbf{R}_1 and \mathbf{R}_2 with a depth $\Delta x(\mathbf{R}_1, \mathbf{R}_2)$ is calculated as:

$$T_R(\mathbf{R}_1, \mathbf{R}_2) = \exp \left(-\frac{\Delta x(\mathbf{R}_1, \mathbf{R}_2)}{x_R} \frac{\int_{\lambda_{min}}^{\lambda_{max}} d\frac{1}{\lambda} (400/\lambda)^4}{\int_{\lambda_{min}}^{\lambda_{max}} d\frac{1}{\lambda}} \right), \quad (11)$$

where $x_R = 2974 \text{ g/cm}^2$.

Mie scattering

$$T_M(\mathbf{R}_1, \mathbf{R}_2) = \exp \left(-\frac{1}{L_M} \int_{\mathbf{R}_1}^{\mathbf{R}_2} dl e^{-h/H_M} \right), \quad (12)$$

where $L_M = 14 \text{ km}$, and $H_M = 1.2 \text{ km}$.

LOWTRAN7.1

Consult lowtran.datacard for the parameter settings (see Sec. IV). Fig. 6 displays LOWTRAN7.1 vertical transition as a function of the light wavelength for various altitudes (starting from 0 to 100).

III. ANALYSIS

Please, note that this study does not take into account electronic inefficiencies, optics, and all other hardware factors. Them should be taken into account in a full simulation chain[17].

Let us define different categories of expected events:

1. (Flevents) Events with fluorescent light
2. (GoldenEvents) Events with fluorescent and cherenkov light
3. (Flonly) Events with fluorescent light but without cherenkov light
4. (Chevents) Events with cherenkov light

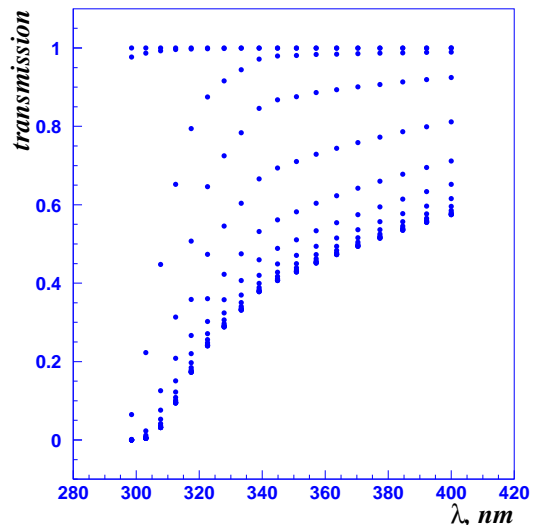


FIG. 6: LOWTRAN vertical transition as a function of the light wavelength for various altitudes (15 values of the altitude starting from 0 to 100 kms with ever doubled stepsize and starting stepsize of 3 m).

5. (Chonly) Events with cherenkov light but without fluorescent light

All these events populate different (E, Θ) parameters space. We apply the following quality cuts for the fluorescence and the cherenkov signals:

$$\begin{aligned} N_f^{max} &> 30 \text{ and } N_{hits} > 25 \\ N_c &> 30 \end{aligned} \quad (13)$$

Here N_f^{max} is the number of photons from the shower maximum per one GTU arrived to EUSO entrance pupil, N_c is the number of cherenkov photons arrived per one GTU to EUSO entrance pupil, and N_{hits} is the number of GTU counts during which the shower is detected. All the results presented below are done assuming $GTU = 0.8 \text{ microsecond}$.

A. Detection Efficiencies

Efficiency is always defined as a ratio of a number of accepted showers over that simulated in a given bin of the variable of interest. Fig. 7 shows the EUSO efficiency as a function of UHECR energy for defined above different categories of expected events. A zoomed version of this plot is shown in Fig. 8. One can see a drastical loss of efficiency for GoldenEvents at $E < 5 \cdot 10^{19} \text{ eV}$, while Flevents show a higher average efficiency with lower threshold.

EUSO efficiency as a function of UHECR zenith angle is displayed in Fig. 9. This plot is averaged over the energy spectrum assuming AGASA spectrum. One can see that on average GoldenEvents are absent at $\Theta > 65^\circ$

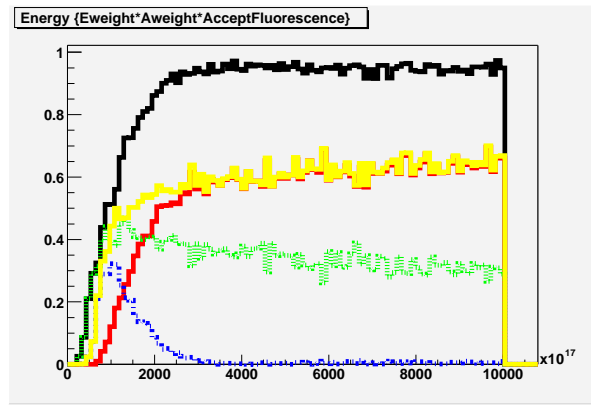


FIG. 7: EUSO efficiency as a function of UHECR energy for defined above different categories of expected events (black line for Flevents, yellow for GoldenEvents, red for Flevents, green for Flonly and blue for Chonly).

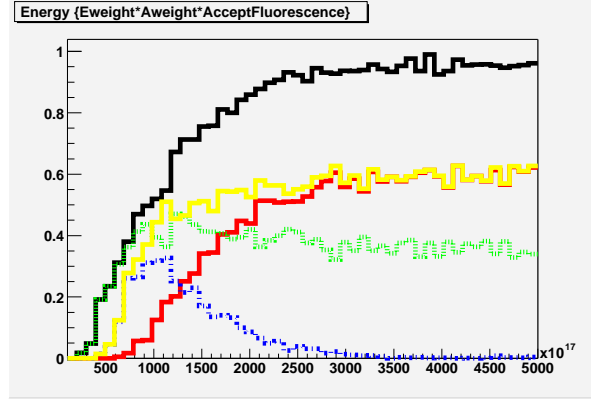


FIG. 8: EUSO efficiency as a function of UHECR energy for defined above different categories of expected events (black line for Flevents, yellow for GoldenEvents, red for Flevents, green for Flonly and blue for Chonly).

which is a very interesting region for an identification of neutrino initiated showers. However Flevents have rather large efficiency at large angles. A two dimensional plot of the EUSO efficiency as a function of UHECR energy and arrival zenith angle is displayed in Fig. 10. One can clearly see that low energy part has a non vanishing efficiency only at significantly large angles where a fraction of golden events is significantly suppressed.

It is also interesting for the focal surface and optics studies to look for the expected distribution of photons as a function of arrival angle. We study this looking for the arrival angle from the shower maximum. Fig. 11 shows expected distribution of arrival angles for Flevents. The observed size of the expected number of events within the arrival angle is due to a larger volume accessible for the showers at larger angles. The efficiency loss at the border stops this size. Therefore, it is highly needed to have optical efficiency high enough at large arrival angles in order to keep the signal as much as possible.

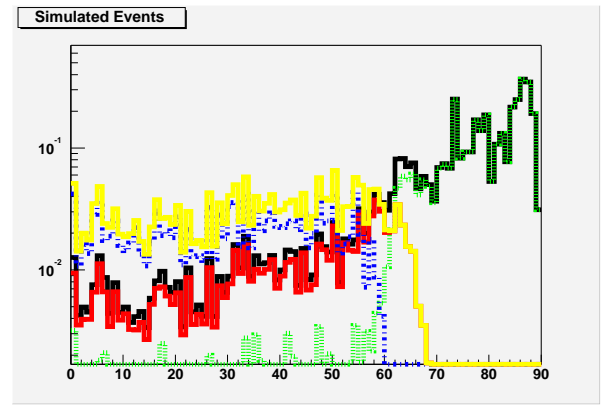


FIG. 9: EUSO efficiency as a function of UHECR zenith angle for defined above different categories of expected events (black line for Flevents, yellow for GoldenEvents, red for Flevents, green for Flonly and blue for Chonly).

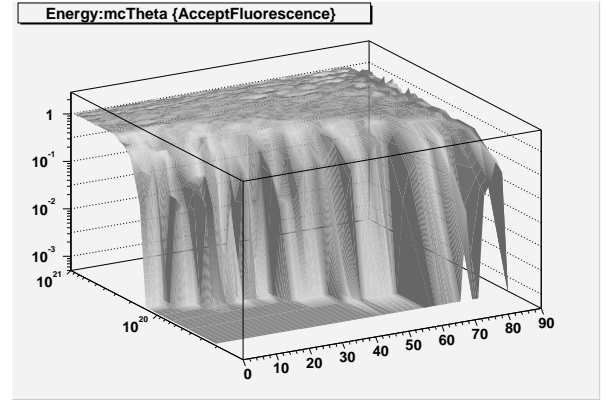


FIG. 10: EUSO efficiency as a function of UHECR energy and zenith angle for Flevents.

B. Photons Arrived to EUSO

The number of photons in the shower maximum depends obviously on the UHECR energy and also it considerably depends on the UHECR zenith angle (see in Fig. 12). There are mainly two reasons for such a dependence:

- the altitude of the maximum of a shower initiated by a nucleus (proton, iron, etc) depends strongly on the zenith angle (see Fig. 13). This implies a smaller absorption of the UV light in the atmosphere for more inclined showers.
- the effective track length corresponding to one GTU time window also depends on the UHECR arrival angles resulting in two times shorter track length for the vertical shower than for the horizontal one (see (9)).

In Figs. 14, 15 I show two slices of Fig. 12 to see clearly these effects. One can see that there is a factor 3 dif-

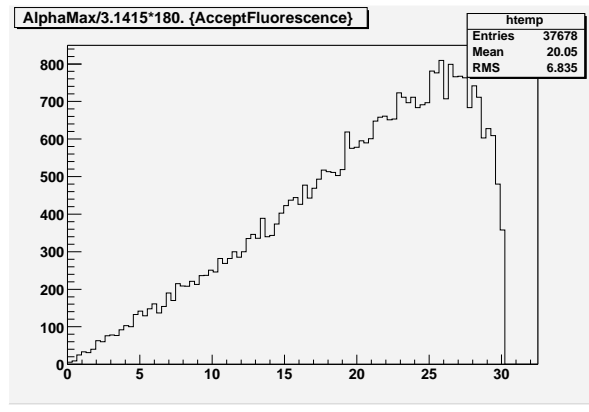


FIG. 11: Expected EUSO distribution of arrival angles for different categories of Flevents. Y axis is arbitrary.

ference between the number of photons from the shower maximum for vertical and horizontal showers.

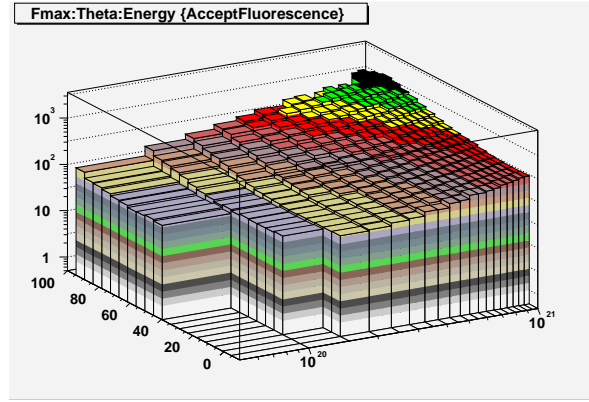


FIG. 12: Expected number of photons from the shower maximum arriving to the EUSO entrance pupil.

Fig. 16 displays the expected total number of photons arriving to the EUSO entrance pupil as a function of UHECR energy and arrival angle. Similarly, in Figs. 17, 18 I show two slices of Fig. 16.

C. Proton/Neutrino discrimination

An idea to discriminate between proton and neutrino initiated showers is relies on their X_{max} distributions. Due to the fact that neutrinos interact uniformly at any depth in the atmosphere their distribution is qualitatively

half of the atmosphere depth for any given zenith angle. However protons start to interact early in the atmosphere thus giving almost the same amount of the atmosphere depth for the shower maximum. Both effects can be seen in Fig. 19. One can conclude that there is a possibility to separate well nucleus and neutrino induced showers near the horizon.

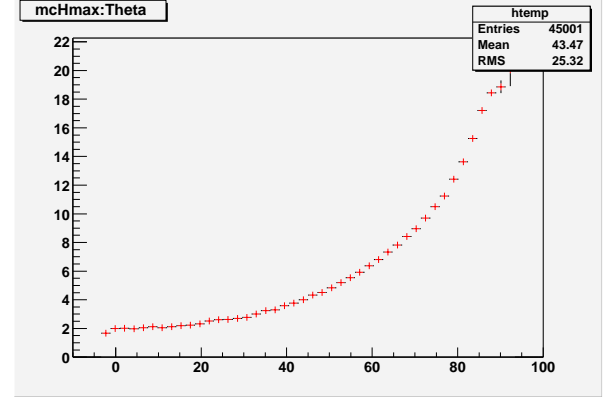


FIG. 13: Altitude of the shower maximum for the proton initiated shower as a function of the UHECR zenith angle.

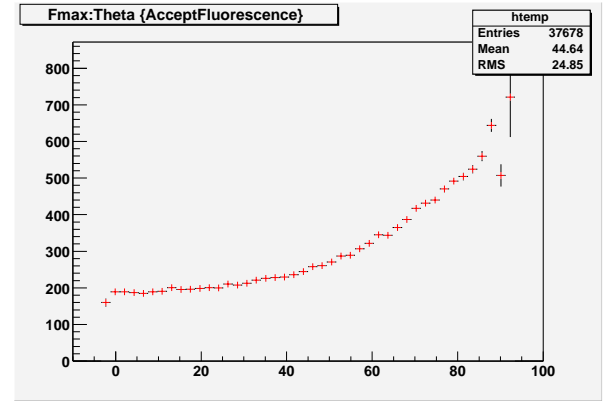


FIG. 14: Expected number of photons from the shower maximum arriving to the EUSO entrance pupil averaged over the AGASA energy spectrum shown as a function of UHECR zenith angle.

D. Expected Statistics

In this section I estimate an expected number of events by EUSO per year of operation basing on AGASA data. The number of events per energy interval dE is given as:

$$dN(E) = 5 \cdot 10^{24} \frac{S}{[m^2]} \frac{Time}{[sec]} DutyCycle \frac{\Omega}{[sr]} \epsilon(E) \frac{dE}{E^3} [eV^2], ;$$

where $S = 1.7120710^{11}$ squared meters is the Earth surface area beneath the EUSO, $Time = 3.1535 \cdot 10^7$ sec-

onds is the number of seconds per year, $DutyCycle =$

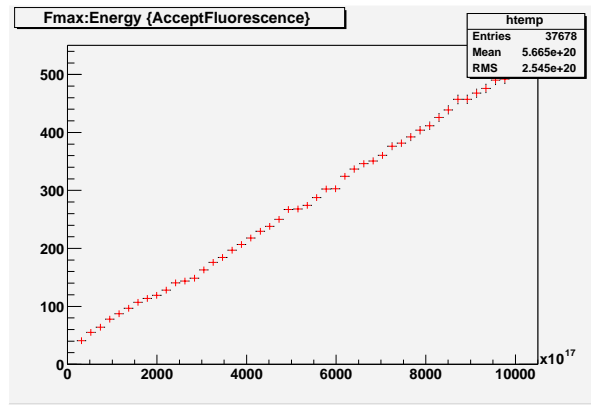


FIG. 15: Expected number of photons from the shower maximum arriving to the EUSO entrance pupil averaged over the UHECR zenith angles shown as a function of UHECR energy.

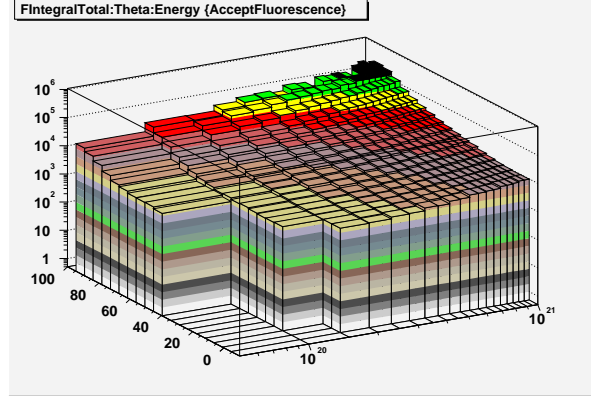


FIG. 16: Expected total number of photons arriving to the EUSO entrance pupil.

0.15 is the effective fraction of day+night time with a background below 400 photons per ns per sr per meter squared[14], $\Omega = \pi$ is the solid angle. S is computed taking into account the Earth sphericity which gives 2% increase in the area compared to the planar Earth consideration. Strictly speaking, solid angle Ω is computed for those events which hits the ground in the EUSO FoV. For Flevents we should not impose such a requirement. We estimated a 4% increase in the solid angle due to this effect (see variable “acc” in CWN output of SLAST in App. A) for proton/iron initiated showers. This number is twice larger for neutrino initiated showers due to a larger contribution of near-horizonal events. However, below we are keeping unique Ω for the sake of simplicity.

The integrated number of events is defined as:

$$N(> E) = \int_E^\infty dN(E).$$

In Fig. 20 I show the expected integrated number of events per year for Flevents (black upper curve) and GoldenEvents (red bottom curve) assuming E^{-3} decrease of the spectrum. Also in this figure are shown

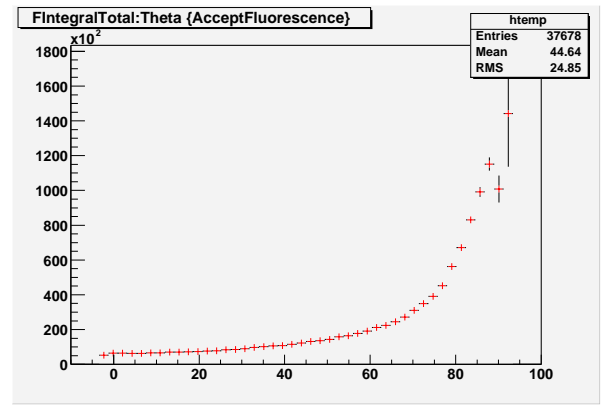


FIG. 17: Expected total number of photons arriving to the EUSO entrance pupil averaged over the AGASA energy spectrum shown as a function of UHECR zenith angle.

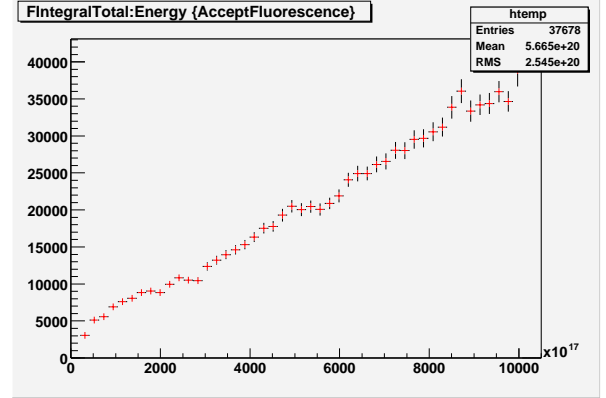


FIG. 18: Expected total number of photons arriving to the EUSO entrance pupil averaged over the UHECR zenith angles shown as a function of UHECR energy.

differential distributions of the above defined events per 10^{19} eV interval. From this plot one can conclude that energy threshold for Golden Events can not be higher than $6 \cdot 10^{19}$ eV with about 200 events per year for them. However, the situation with Fluorescent events is somehow better: the energy threshold is $2 \cdot 10^{19}$ eV with more than 1000 events per year. Please, note again, that these numbers are obtained ignoring effects of optics and electronics. However, our preliminary studies with ESAF and SLAST as its light generator shows that these effects are very important. These points will be discussed in a subsequent note and are beyond the scope of this document.

IV. STEERING THE SIMULATIONS

SLAST is a package of FORTRAN77 programs using CERNLIB functions, therefore cernlib library (see <http://cernlib.web.cern.ch/cernlib/>) must be installed.

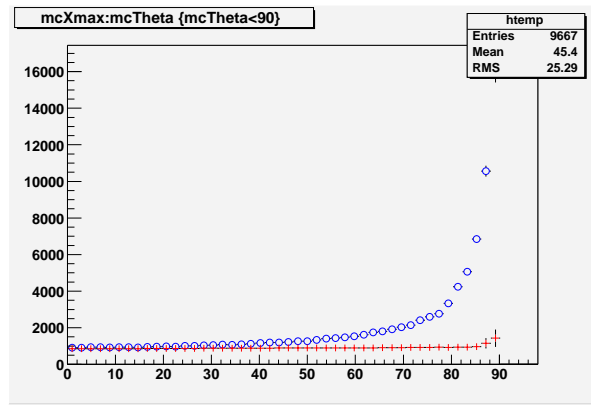


FIG. 19: X_{max} mean values for proton and neutrino initiated showers.

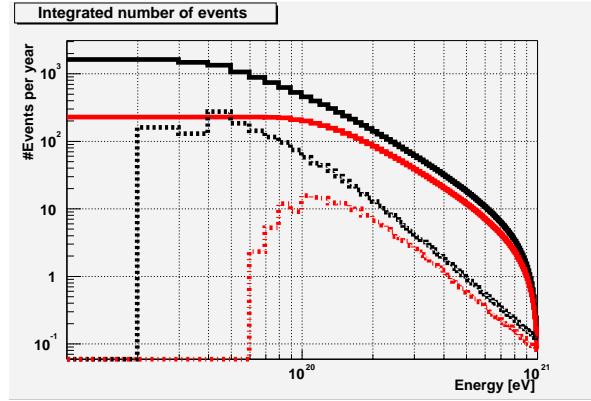


FIG. 20: Expected integrated number of events per year for Flevents (black solid curve) and GoldenEvents (red solid curve) assuming E^{-3} spectrum. The corresponding dashed and dot-dashed curves are for the differential distributions of the above defined events per 10^{19} eV interval.

A. Code maintenance and general agreements

The SLAST sources are stored at Lyon Computer Center under CVS (web access <https://cvs.in2p3.fr/eusof/>) and they are free of charge for anybody interested in a fast generation of extensive atmospheric showers and fluorescent and cherenkov light signals. The author takes care to improve the code and fix bugs. However SLAST is NO WARRANTY software and the author does not take any responsibility for any damage of your software or hardware happened using SLAST.

The sources can be downloaded in a precompiled form or via CVS checkout. I advise you always to use the last possibility thus having always the most recent and most advanced version.

CVS downloading

1. Use ssh access. Add the following lines into your .ssh/config file:

```
Host cvs.in2p3.fr
```

```
Port 2222
User euso
PasswordAuthentication yes
RSAAuthentication no
PubkeyAuthentication no
ForwardX11 no
ForwardAgent no
```

2. Set environment:

```
setenv CVSR00T euso@cvs.in2p3.fr:/cvs/eusof
setenv CVS_RSH ssh
```

3. Type:

```
cvs checkout slast
```

Your comments are welcome: (naumov@lapp.in2p3.fr)

B. Compilation

After you have successfully downloaded the sources you should compile the sources and make first installation run:

1. Compilation:

```
make
```

Normally it should give on your screen many lines of compilation but at the end you should see something like:

```
*****
* slast.exe.Linux
* is up to date.
*****
```

2. Installation:

```
geninst
```

This will take quite a lot of time to compute all necessary things. However you should do it only once and later your simulation will be rather fast. The most time consuming part here is LOWTRAN7.1. It can take up to 10 hours (depending on your PC's clock) to calculate all needed histograms. You can save your time if you contact me to provide the needed file with all histos already computed. By technical reasons this file can not be stored under CVS.

Once you have successfully downloaded and installed the package you may find interesting to make some simulations. The idea behind SLAST which we find useful is to set the simulation parameters in special ascii files called `global.datacard` and `lowtran.datacard` thus avoiding recompilation. These datacards are stored in a directory “datacards” inside SLAST. There you may find the following files:

1. `datacard.install` (installation datacard, normally this is hidden from user)
2. `datacard.euso` (datacard with detector parameters relevant for EUSO)
3. `datacard.klpve` (datacard with detector parameters relevant for KLYPVE)
4. `datacard.tus` (datacard with detector parameters relevant for TUS)
5. `lowtran.datacard` (datacard with LOWTRAN7.1 parameters)

Ready to start:

1. Linking datacards to your current directory:

```
ln -sf datacards/datacard.euso global.datacard
ln -sf datacards/lowtran.datacard .
```

2. Edit these datacard files as you need. The parameters of `global.datacard` are explain in Tab. I. The parameters of `lowtran.datacard` are commented inside (see also LOWTRAN7.1 manual).

Set up number of events you would like to generate (NEVT keyword), Θ and ϕ intervals (THET and PHI keywords), energy interval (EINT keyword) and type of the particle (TYPE keyword). SLAST uses the following convention:

- if $TYPE < 1000$ than TYPE is the atomic number of the incident nucleus.
 - $TYPE = 1001$ corresponds to neutrino interactions.
3. Run: `Linux/slast.exe.Linux` (if you are using another UNIX type system, than SLAST will automatically determine it and will create the corresponding directory with slast libraries and executables. Say, at DEC ALPHA station you may see OSF1 directory with `slast.exe.OSF1` executable inside).

There are two output formats of SLAST:

1. PAW Column Wise Ntuple, stored by default in “events.cwn” file,
2. ESAF input format.(this is obsolete today since SLAST is now inside ESAF and can be run directly generating showers on fly)

In Tab. II we display all CWN variables and their meaning.

Acknowledgments

I am grateful to Pierre Colin, Vadim A.Naumov, Patrick Nedelec for usefull discussions and help.

TABLE I: Global datacard parameters

PARAMETERS	EXPLANATION
ERAD	EARTH RADIUS IN KM
ISSF	Space Telescope Radius Vector from the GROUND, (km,km,km)
FOV	FIELD OF VIEW OF THE DETECTOR (in degrees)
ARES	ONE PIXEL ANGULAR RESOLUTION (in radians)
NPMT	NUMBER OF PIXELS in one dimension
SDIA	Entrance Pupil diameter
WAVE	MINIMAL AND MAXIMAL VALUES OF THE WAVELENGTH BAND (nm, nm)
DOCH	Calculate (1) or not (0) the Cherenkov signal
DOFL	Calculate (1) or not (0) the Fluorescent signal
ATMO	CHOSE THE ATMOSPHERE profile
TEMP	TEMPERATURE OF THE ATMOSPHERE IN THE ISOTHERMIC MODEL (in K)
TRAN	ATMOSPHERE TRANSITION
ALBE	UV Earth ALBEDO
GTU	GTU (in msec)
QEFF	QUANTUM EFFICIENCY OF PMT'S
CURV	ATMOSPHERE SPERICITY
THRE	DETECTOR THRESHOLD FOR TE NUMBER OF PHOTONS
RUN	RUN NUMBER
NEVT	NUMBER OF EVENTS TO GENERATE
RINT	FIRST INTERACTION POINT RADIUS VECTOR (x,y,z) in km (valid only for 1 event)
THET	THETA ANGLE INTERVAL OF INCOMING PARTICLE (in degrees)
PHI	PHI ANGLE INTERVAL OF INCOMING PARTICLE (in degrees)
EINT	ENERGY INTERVAL OF INCOMING PARTICLE (in eV)
TYPE	ATOMIC MASS OF THE INCOMING PARTICLE (FOR NUCLEI)
ZNUC	CHARGE OF THE INCOMING PARTICLE (FOR NUCLEI)
INTE	(ANTI) NEUTRINOS: CC or NC
QCDC	QCD CORRECTIONS: LO, NLO
DIST	ENERGY DISTRIBUTION OF ELECTRONS IN THE SHOWER
SHOW	A SHOWER PARAMETRIZATION
POWE	INCOMING PARTICLE'S ENERGY POWER CONSTANT E**(-POWER)
OUTF	RANDOM OR MEAN VALUES OF FLUORESCENT PHOTONS IN THE OUTPUT
OUTC	RANDOM OR MEAN VALUES OF CHERENKOV PHOTONS IN THE OUTPUT
ESAF	PRODUCE (1) OR NOT (0) ESAF OUTPUT

APPENDIX A: COLUMN WISE NTUPLE STRUCTURE

-
- [1] J. W. Cronin *et al.*, FERMILAB-PROPOSAL-881
[2] O. Catalano, Nuovo Cim. **24C**, 445 (2001).
[3] B. A. Khrenov *et al.*, AIP Conf. Proc. **566**, 57 (2000).
[4] Vadim A. Naumov, private communication
[5] V.A. Naumov and T.S. Sinegovskaya, Yad. Fiz. 63, 2020 (2000) [Phys. Atom. Nucl. 63, 1927 (2000)].
[6] R. Basu, D. Choudhury and S. Majhi, JHEP **0210**, 012 (2002) [arXiv:hep-ph/0208125].
[7] M.V. Tognetti, Tesi in Laurea in Fisica, Firenze, (2000)
[8] F. Kakimoto, E. C. Loh, M. Nagano, H. Okuno, M. Teshima and S. Ueno, Nucl. Instrum. Meth. A **372**, 527 (1996).
[9] G. Davidson and R.O'Neil, J.Chem.phys. 41 3946 (1964)
[10] B.Rossi and K.Greisen, Rev.Mod.Phys., 13, 240 (1941)
[11] N. P. Ilina, N. N. Kalmykov and V. V. Prosin, Sov. J. Nucl. Phys. **55**, 1540 (1992) [Yad. Fiz. **55**, 2756 (1992)].
[12] N.N.Kalmykov and S.S.Ostapchenko, Sov.J.Nucl.Phys. **50**, 315 (1989)
[13] A.M.Hillas, J.Phys.G:Nucl.Phys.8, 1461 (1982)
[14] P.Colin, EUSO-SIM-007
[15] The needed depth can be easily accumulated traversing water and/or rock thus giving subhorizontal showers. This is foreseen but not yet implemented into SLAST.
[16] taken from <http://physics.nist.gov>
[17] Now SLAST is implemented into ESAF package as a light generator. We are studying effects of the optics and the trigger on the expected statistics

TABLE II: SLAST output CWN variables

Variable	TYPE	EXPLANATION
run	Integer	run number of your job
event	Integer	Event number
type	Integer	Type of the incident particle
Energy	Real*4	Log(EINT/eV)
ew	Real*4	Weight corresponding to $E_{int}^{-\gamma}$
Xint	Real*4	X coordinate of the first interaction point (km)
Yint	Real*4	Y coordinate of the first interaction point (km)
Zint	Real*4	Z coordinate of the first interaction point (km)
Thet	Real*4	Θ - Incident zenith angle (deg.)
Ph	Real*4	ϕ - Azimuthal angle (deg.)
observ	Real*4	Local ground altitude above sea level (km)
cloud	Real*4	Cloud altitude (km)
qeff	Real*4	PMT quantum efficiency
XG	Real*4	X coordinate of the shower impact point on the ground (km)
YG	Real*4	Y coordinate of the shower impact point on the ground (km)
ZG	Real*4	Z coordinate of the shower impact point on the ground (km)
acc	Real*4	Acceptance: 1 - hits the ground in FOV, 2 - hits the ground outside FOV, 3 - does not hit the ground
x1	Real*4	Atmosphere depth in the first interaction point (g/cm^2)
fimax	Real*4	Maximal number of fluorescent photons per one GTU without attenuation
fltmax	Real*4	Maximal number of fluorescent photons per one GTU with LOWTRAN7.1 attenuation
chmax	Real*4	Maximal number of cherenkov photons per one GTU without attenuation
chttot	Real*4	Maximal number of cherenkov photons per one GTU with LOWTRAN7.1 attenuation
ftot	Real*4	Total number of fluorescent photons without attenuation
flttot	Real*4	Total number of fluorescent photons with LOWTRAN7.1 attenuation
chtot	Real*4	Total number of cherenkov photons without attenuation
chttot	Real*4	Total number of cherenkov photons with LOWTRAN7.1 attenuation
ns	Integer	Number of GTU hits of the shower
Ne	Real*4	List of number of electrons corresponding to each GTU hit
depthr	Real*4	List of atmospheric depth - x_1 along the shower path (g/cm^2)
length	Real*4	List of length of the shower along the shower path (km)
age	Real*4	List of the shower age
height	Real*4	List of the shower altitude
nf	Integer	Number of GTU hits of the shower
Nfl	Real*4	List of number of fluorescent photons without attenuation
Nflt	Real*4	List of number of fluorescent photons with LOWTRAN7.1 attenuation
wave_fl	Real*4	List of mean wavelengths of the fluorescent photons (obsolete)
time_fl1	Real*4	List of arrival time of fluorescent photons assuming speed of light in the vacuum
time_fl2	Real*4	List of arrival time of fluorescent photons taking into account $n \neq 1$
Tr_fl	Real*4	List of Rayleigh attenuation coefficients for fluorescent light
Tm_fl	Real*4	List of Mie attenuation coefficients for fluorescent light
mxfl	Real*4	List of X PMT cells hitted by the fluorescent light
myfl	Real*4	List of Y PMT cells hitted by the fluorescent light
angxfl	Real*4	List of α_x arrival angle of the fluorescent light
angyfl	Real*4	List of α_y arrival angle of the fluorescent light
nc	Integer	Number of GTU hits of the shower
Nch	Real*4	List of number of cherenkov photons without attenuation
Ncht	Real*4	List of number of cherenkov photons with LOWTRAN7.1 attenuation
Nchtot	Real*4	List of accumulated number of cherenkov photons without attenuation
Nchttot	Real*4	List of accumulated number of cherenkov photons with LOWTRAN7.1 attenuation
time_ch1	Real*4	List of arrival time of cherenkov photons assuming speed of light in the vacuum
time_ch2	Real*4	List of arrival time of cherenkov photons taking into account $n \neq 1$
Tr_ch	Real*4	List of Rayleigh attenuation coefficients for cherenkov light
Tm_ch	Real*4	List of Mie attenuation coefficients for cherenkov light
mxch	Real*4	List of X PMT cells hitted by the cherenkov light
mych	Real*4	List of Y PMT cells hitted by the cherenkov light
angxch	Real*4	List of α_x arrival angle of the cherenkov light
angych	Real*4	List of α_y arrival angle of the cherenkov light

```

*****
* Ntuple ID = 1      Entries = 1      EVENT
*****
* Var numb * Type * Packing *      Range      * Block * Name *
*****
*      1 * I*4 *          *          * GENINFO * run
*      2 * I*4 *          *          * GENINFO * event
*      3 * I*4 *          *          * GENINFO * type
*      4 * R*4 *          *          * GENINFO * Energy
*      5 * R*4 *          *          * GENINFO * ew
*      6 * R*4 *          *          * GENINFO * Xint
*      7 * R*4 *          *          * GENINFO * Yint
*      8 * R*4 *          *          * GENINFO * Zint
*      9 * R*4 *          *          * GENINFO * Thet
*     10 * R*4 *          *          * GENINFO * Ph
*     11 * R*4 *          *          * GENINFO * observ
*     12 * R*4 *          *          * GENINFO * cloud
*     13 * R*4 *          *          * GENINFO * qeff
*     14 * R*4 *          *          * GENINFO * XG
*     15 * R*4 *          *          * GENINFO * YG
*     16 * R*4 *          *          * GENINFO * ZG
*     17 * R*4 *          *          * GENINFO * acc
*     18 * R*4 *          *          * GENINFO * x1
*     19 * R*4 *          *          * GENINFO * flmax
*     20 * R*4 *          *          * GENINFO * fltmax
*     21 * R*4 *          *          * GENINFO * chmax
*     22 * R*4 *          *          * GENINFO * chtmax
*     23 * R*4 *          *          * GENINFO * fltot
*     24 * R*4 *          *          * GENINFO * flttot
*     25 * R*4 *          *          * GENINFO * chtot
*     26 * R*4 *          *          * GENINFO * chttot
*      1 * I*4 *          * [0,500] * SHOWER * ns
*      2 * R*4 *          *          * SHOWER * Ne(ns)
*      3 * R*4 *          *          * SHOWER * depthr(ns)
*      4 * R*4 *          *          * SHOWER * length(ns)
*      5 * R*4 *          *          * SHOWER * age(ns)
*      6 * R*4 *          *          * SHOWER * height(ns)
*      1 * I*4 *          * [0,500] * FLUOR * nf
*      2 * R*4 *          *          * FLUOR * Nfl(nf)
*      3 * R*4 *          *          * FLUOR * NflT(nf)
*      4 * R*4 *          *          * FLUOR * wave_fl(nf)
*      5 * R*4 *          *          * FLUOR * time_fl1(nf)
*      6 * R*4 *          *          * FLUOR * time_fl2(nf)
*      7 * R*4 *          *          * FLUOR * Tr_fl(nf)
*      8 * R*4 *          *          * FLUOR * Tm_fl(nf)
*      9 * I*4 *          *          * FLUOR * mxfl(nf)
*     10 * I*4 *          *          * FLUOR * myfl(nf)
*     11 * R*4 *          *          * FLUOR * angxfl(nf)
*     12 * R*4 *          *          * FLUOR * angyfl(nf)
*      1 * I*4 *          * [0,500] * CEREN * nc
*      2 * R*4 *          *          * CEREN * Nch(nc)
*      3 * R*4 *          *          * CEREN * NchT(nc)
*      4 * R*4 *          *          * CEREN * Nchtot(nc)
*      5 * R*4 *          *          * CEREN * NchTtot(nc)
*      6 * R*4 *          *          * CEREN * time_ch1(nc)
*      7 * R*4 *          *          * CEREN * time_ch2(nc)
*      8 * R*4 *          *          * CEREN * Tr_ch(nc)
*      9 * R*4 *          *          * CEREN * Tm_ch(nc)
*     10 * I*4 *          *          * CEREN * mxch(nc)
*     11 * I*4 *          *          * CEREN * mych(nc)
*     12 * R*4 *          *          * CEREN * angxch(nc)
*     13 * R*4 *          *          * CEREN * angych(nc)
*****

```